

Stellar Masers: Observations and Simulations

E.M.L. Humphreys¹ and M. D. Gray²

¹ Harvard-Smithsonian Center for Astrophysics, 60 Garden Street, Cambridge, MA 02138, USA

² Physics Department, UMIST, PO Box 88, Manchester M60 1QD, UK

Abstract. Maser lines provide tools for the study of circumstellar envelopes (CSEs) of oxygen-rich, red giant stars. VLBI allows the imaging of stellar maser emission down to sub-milliarcsecond scales. Such observations reveal asymmetry, inhomogeneity and apparent clumpiness in the extended atmosphere and surrounding envelope of the stars. Inhomogeneity from $2R_*$ out may result from 'shadowing' due to dust formation, leading to cooler regions in the CSE. Closer in, investigation of whether inhomogeneity in the extended atmosphere originates from stellar surface features such as stellar hot/coolspots is needed. Maser studies additionally place constraints on processes that are seldom included in stellar hydrodynamical models, e.g., magnetic fields, rotation. Here, I discuss observational data on stellar masers, stellar maser simulations and the implications for our understanding of red giant stars.

1. Introduction

Stellar masers (SiO, H₂O and OH) provide an excellent method of studying the CSEs of M-type supergiants and of red giants on the Asymptotic Giant Branch (AGB). Firstly, masers from different molecules require different pumping conditions. Hence they probe different regions of the extended CSE built up by long-period variables such as Miras, Semi-Regulars and OH/IR stars. Since each molecule can yield maser emission from different transitions, radiative transfer modeling provides good constraints on the physical conditions in each of the regions. Secondly, since masers are compact, of high brightness temperature, the emission is ideal for study using VLBI. For example, SiO masers at 43 GHz can now be imaged with sub-mas angular resolution and with high velocity resolution (0.1 kms⁻¹). Finally, maser emission varies during the stellar pulsation cycles of AGB stars. Thus time-series observations of stellar masers provide an unprecedented view of the gas dynamics and physical conditions surrounding mass-losing stars as a function of stellar phase. Below I outline observational data on stellar masers, starting from emission originating nearest to the photosphere and working outwards, some stellar maser simulations and a brief outlook for the future.

2. SiO Masers

SiO maser emission has been detected in a range of rotational transitions, from $J = 1 - 0$ (43 GHz) up to at least $J = 10 - 9$ (430 GHz), within vibrational states $\nu = 0$ to $\nu = 4$ (e.g. Pardo et al. 1998; Bieging et al. 2000). Long-term monitoring studies of selected transitions have been made e.g., by Pardo et al. (2004) and Alcolea et al. (1999). Maser and thermal emission originating from the ground vibrational state has recently been studied by Boboltz & Claussen (2004).

2.1. VLBI Studies

At the resolution of the VLBA, SiO maser emission is distributed in a ring-like structure of emitting spots, within a

few stellar radii (several AU) of the assumed stellar position. Diamond et al. (1994) were the first to resolve such emission structure for $\nu = 1 J = 1 - 0$ emission towards TX Cam and U Her and show that stellar SiO masers amplify tangentially. Tangential amplification is the norm for SiO masers since high radial velocity gradients in the extended atmosphere region severely limit radial amplification path lengths. Earlier, EVN observations had already placed limits on the size of stellar SiO maser emission spots at $\sim 10^{12}$ cm (Colomer et al. 1992). Some tens of percent of the single-dish maser flux are missing in the high spatial resolution observations. More extended emission structures, resolved out on VLBA baselines, must also be present and require investigation.

Since then, maser rings have been found to be a common phenomenon, via imaging at 43 and 86-GHz towards several stars - (for example Greenhill et al. 1995 for $\nu = 1 J = 1 - 0$ masers in VX Sgr; Boboltz et al. 1997 for $\nu = 1 J = 1 - 0$ masers in R Aqr; Doeleman et al. 1998 for $\nu = 1 J = 2 - 1$ masers in VX Sgr; Desmurs et al. 2000 for $\nu = 1$ & $2 J = 1 - 0$ masers in TX Cam & IRC+10011; Yi et al. 2002 for $\nu = 1$ & $2 J = 1 - 0$ masers in TX Cam & R Cas; Phillips et al. 2003 for $\nu = 1 J = 1 - 0$ & $J = 2 - 1$ in R Cas). A study of 9 stars has recently been made by Cotton et al. (2004) using the VLBA. The stars were observed in the $\nu = 1$ and $\nu = 2 J = 1 - 0$ transitions for 1 - 4 epochs each during one year (total intensity and linear polarization). As expected, SiO emission was found to be largely confined to rings that are smaller than the inner radius of the circumstellar dust shells (as reported by Danchi et al. 1994). Such observations confirm the location of SiO masers in the extended atmosphere between the stellar photosphere and the inner radius of the circumstellar dust shell (see also Greenhill et al. 1995). In this way energy and chemical requirements for SiO are fulfilled: close to the star in warm, dense regions for populating energy levels >1800 K above ground state, and placing masers in regions of high gas phase SiO abundance, within the radius at which dust condensation takes place. SiO masers are believed to lie just

beyond a stellar “radio photosphere”, at around $2R_*$ (Reid & Menten 1997).

All these data indicate the inhomogeneity of the extended atmosphere, the cause of which is unknown. Proposed mechanisms include:

- The formation of maser clumps via thermal instabilities, which result from infrared band ‘runaway’ cooling by SiO and CO (Cuntz & Muchmore 1994). However, recent calculations suggest that this is unlikely (Woitke, private communication).
- Observations of the stellar disk itself could hold the key. The spherically-symmetric, homogeneous picture presented by stellar models of mass-loss is in conflict with many observations of AGB stars. These show that the stellar disk shows significant deviations from circular symmetry, and that there is an uneven brightness distribution over the stellar disk (Tuthill et al. 1997 and references therein). These asymmetries may be intimately connected to the presence of convective cells on the stellar surface. Such phenomena were first suggested by Schwarzschild (1975), who speculated that granulation of the type observed for the sun would also occur in AGB stars. Schwarzschild showed that, for AGB stars, the convective features would grow so large that only a few could exist on the stellar surface at one time. The resulting large surface temperature variations and accompanying brightness fluctuations would mean that the emitted radiation would become highly anisotropic, leading to polarization of the light scattered by circumstellar dust, as observed. They would also lead to asymmetries in the formation of dust, since it would condense nearer to the star over cooler regions than over the hotter regions, and of masers. Unfortunately recent high resolution imaging of Betelgeuse (see Perrin et al. 2004) has found a distinct lack of evidence for large convective cells on the star, and has led to papers such as “Giant Convection Cells, Where Are You?” (Gray 2003). Current data are consistent with several hundreds of smaller-scale cells instead.
- Another route to clump formation could be the magnetohydrodynamical Parker instability (see Hartquist & Dyson 1997). This would require a magnetic field of around 50 G however.
- The extended atmosphere region is also likely to be highly turbulent. The significance for masers is that only a limited number of lines of sight are available in a turbulent medium for masers to propagate for substantial lengths and therefore to build up high intensities. This could be an important contributory feature in causing intense masers to form an incomplete ring of structures about the central star.

2.2. Multi-Transition Observations

SiO maser ring radii can vary with transition. Cotton et al. (2004) show that the *mean ring diameters* of $\nu = 1 J = 1 - 0$ and $\nu = 2 J = 1 - 0$ differ by typically 2 – 3 mas (their Table 5). In previous observations towards a few red giants, there is a clear average spatial separation between the $\nu = 1 J = 1 - 0$ and the $\nu = 2 J = 1 - 0$ maser rings, when observed at high

enough spatial resolution (~ 0.5 mas). The separation is < 0.5 AU, the $\nu = 2$ masers lying inside the corresponding $\nu = 1$ features (Desmurs et al. 2000; Yi et al. 2002). Significant changes to this picture can occur as a function of stellar phase, see below.

2.3. Time Variations in the Structure of SiO Maser Emission

Maser rings are not static, diameters change with stellar phase. The first proper motion measurements showed the maser ring in the symbiotic Mira R Aqr in contraction as the intensity of the ring faded, with an average velocity of $\sim 4 \text{ kms}^{-1}$. These observations covered around a quarter of the stellar cycle ($\cong 100$ days) and were consistent with infall under gravity. The most complete multi-epoch data towards a single source is the monitoring of the $\nu = 1 J = 1 - 0$ masers in TX Cam over > 1.5 cycles by Diamond & Kemball (2003). Both infalling and outflowing gas is observed, but *expansion dominates the dynamics* between $\phi 0.7 - 1.5$. For example, over a nine month period in 1998, the ring had expanded by $> 10\%$ in some directions (Diamond & Kemball 1999, 2001). Some of the maser components move outwards with a constant velocity of $\sim 10 \text{ kms}^{-1}$. These observations provide strong evidence for shocks. Disruption to the maser ring appears to occur at minimum maser light (Diamond, private communication). Around this time a new maser ring is observed to form inside the radius of the previous ring.

Cotton et al. (2004) find that maser rings vary by significantly different amounts for different sources during their observations - 20 % for α Ceti $\nu = 1 J = 1 - 0$, whilst there is remarkably small variation for ring diameter in U Ori. Cotton et al. find that the $\nu = 2 J = 1 - 0$ ring can rarely expand to have a larger diameter than the $\nu = 1$ counterpart in the same source (at one epoch in 2 sources only, both of which are part of binaries).

2.4. Polarization Structure

In Cotton et al. (2004), there are only a few cases in the 9 stars in which the polarization of the inner portion of the ring is tangential. In fact, “*there is no prominent pattern that is a persistent feature in the polarization of any of the stars observed*”.

Yet in earlier VLBA data for TX Cam, there is a highly ordered polarization structure. Most SiO maser spots are linearly polarized in a direction which is tangential to the maser ring (Kemball & Diamond 1997, Diamond & Kemball 2001; Desmurs et al. 2000). The degree of linear and circular polarization varies substantially between components. When averaged over the shell, linear polarization is at around the 30 % level and circular polarization is $\sim 3\%$. However, Diamond & Kemball (2001) show clearly that the south east portion of the ring can also display a smaller, additional circular linear polarization structure, the source of which is unknown. A speculative origin for this feature is that it could be marking out a “local small-scale dynamo” (see e.g. Dorch 2004).

Ambiguity in the interpretation of SiO maser polarization arises as SiO is non-paramagnetic. Zeeman splitting would be smaller than the SiO thermal linewidth, for gas kinetic temperatures say around 1500 K, unless the magnetic field is of the order $\sim 10^3$ G. Taking a Zeeman interpretation, the linear polarization pattern provides an indication of the magnetic field structure and the observed circular polarization implies a magnetic field strength of 5 – 10 G (Kemball & Diamond 1997; Elitzur 1996). For a field of this strength, the magnetic pressure will greatly exceed the gas thermal pressure for the conditions expected in the SiO maser zone (see Barvainis et al. 1987). In this case the magnetic field would be the dominant force in determining the kinematics of maser cells. Blackman et al. (2001) describe how strong magnetic fields can be produced via a dynamo at the interface between a rapidly rotating core and a more slowly rotating stellar envelope in AGB stars. Herpin et al. (2003) measured the average magnetic field in the line-of-sight to the SiO maser zone for 100 AGB stars and found values from 1 – 32 G, with an average value of 9 G.

Under the non-Zeeman interpretation, the observed linear polarization is due to anisotropy in the radiative pumping of SiO masers by stellar photons (Western & Watson 1983). In this scenario the quantization axis is provided by the pumping process itself, the radial direction of the stellar IR pump photons, rather than by a magnetic field. Tangential polarization then arises as molecules rotating in the tangential plane preferentially absorb the stellar photons. This mechanism is clearly described by Desmurs et al. (2000). Given the observed linear polarization, Wiebe & Watson (1998) show that the circular polarization can be produced if the direction of a magnetic field of only > 30 mG changes in orientation along the line of sight.

See Gray (2003) for a comparison of maser polarization theories.

2.5. Rotation in the SiO Maser Zone

Interpretation for rotation in the SiO maser zone has been made for a few stars - NML Cyg (Boboltz & Marvel 2000); IK Tau (Boboltz & Diamond 2000); R Aqr (Hollis et al. 2001) and VX Sgr (Doeleman et al. 1998). Towards the supergiant NML Cyg, the $\nu = 1 J = 1 - 0$ spectrum shows an unusual double-peaked profile, which in conjunction with the spatial velocity distribution, could be interpreted as rotation of the maser shell with a velocity of $V_m \sin i \approx 11 \text{ km s}^{-1}$. Cotton et al. (2004) find clear evidence in R Aqr for an equatorial disk similar to that reported by Hollis et al. and rotation is possibly also detected in S Coronae Boralis.

3. H₂O Masers

The most well-studied H₂O maser line is that at 22 GHz arising from the $6_{16} \rightarrow 5_{23}$ transition in the ground vibrational state of ortho-H₂O. The upper level of this transition lies at an E_u/k of ~ 650 K. MERLIN (milli-arcsecond resolution; velocity resolution 0.1 km s^{-1}) and VLA interferometry data have provided the evidence that the stellar H₂O maser emission at 22 GHz is located in a shell expanding from AGB stars (e.g. Reid &

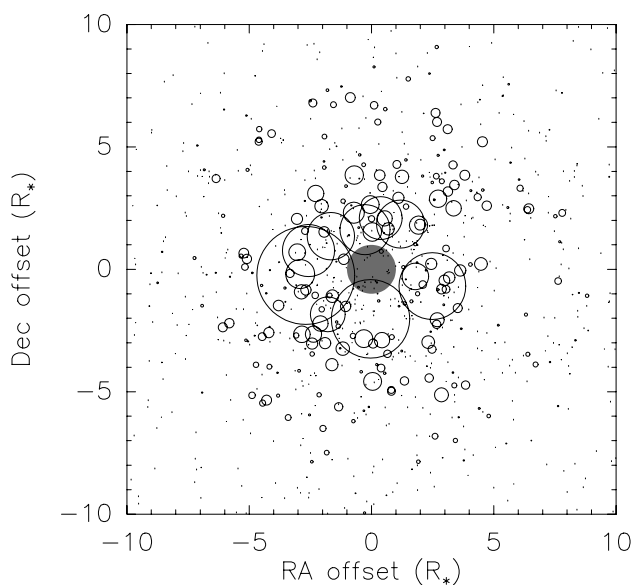


Fig. 1. 22 GHz H₂O maser emission at a single stellar phase. Intensities of the masers are linearly proportional to the diameters of the black circles shown. Circles are centred on the maser projected coordinates. The grey disk represents the stellar disk of mean radius 1.1 AU.

Menten 1990; Bowers & Johnston 1994; Yates et al. 1994; Colomer et al. 2000). The shell appears clumpy and incomplete at these resolutions. Emission originates from the inner parts of the CSE of Mira-type stars, from regions out to $\sim 10^{15}$ cm, which are comparable in extent to those in which dust grains form and grow, and in which the expanding envelope has not yet reached terminal velocity. 22 GHz masers are believed to probe stellar gas in which acceleration away from the star takes place via radiation pressure on dust and subsequent gas-grain collisions (Chapman & Cohen 1986). Other H₂O masers are commonly found in the evolved circumstellar environment. For example, maser emission at 321, 325 and 183 GHz (Menten et al. 1990; Menten & Melnick 1991; Yates et al. 1995; González-Alfonso et al. 1998).

Inhomogeneity in the H₂O maser zone could be related to dust-formation. Woitke et al. (2000) find the initial formation of dust, at least in C-type Miras, provides regions in the CSE that are shadowed from stellar radiation. Temperatures in the shadows drop to a few hundred kelvin lower than the rest of the gas at the same radius. These regions then become conducive to further dust formation and can form dust clouds, clumps and spokes on stellar radius scales, and perhaps masers. Such morphology for dust has been observed e.g., by Tuthill et al. (1999) who find that for some stars, "...dramatic dust plumes and clumps dominate the morphology of the circumstellar environment at a scale of a few stellar radii....".

22 GHz masers result from collisional excitation followed by radiative decay, thus maser components are expected to lie in a shell whose inner and outer boundaries are determined by collision rates. In theory, at the inner boundary, collision rates quench the maser inversion by thermalising the energy level populations of molecules in the gas. Whilst at the outer bound-

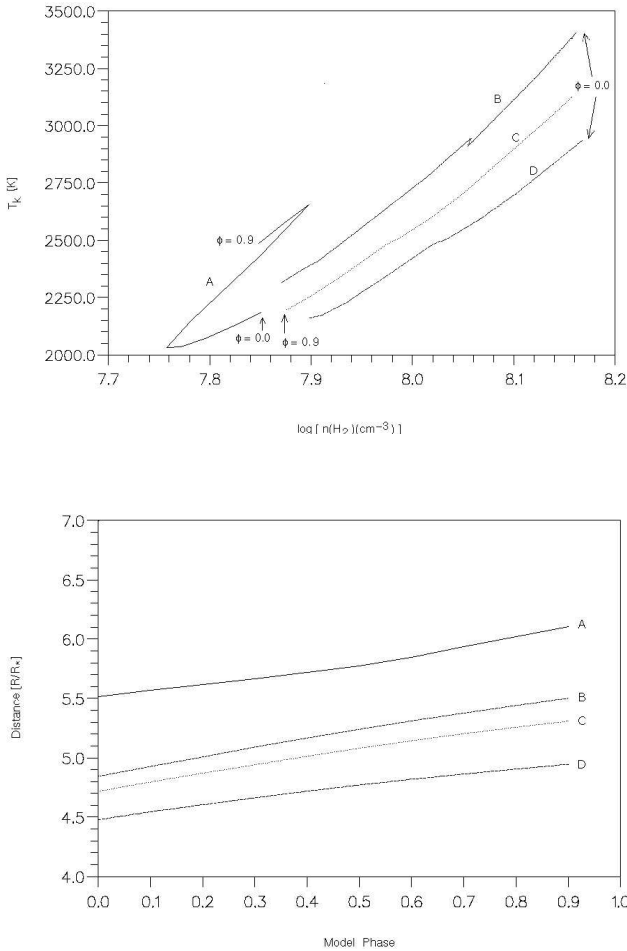


Fig. 2. Temporal attributes: a) (top) Physical conditions experienced by four bright 22 GHz components throughout a stellar pulsation cycle of 332 days ($\equiv \Delta\phi = 1.0$); b) (bottom) the motions of these components within the CSE.

ary collision rates are too low to pump the 22 GHz inversion. In addition, photolysis by the interstellar radiation field acts to reduce H_2O abundance in the outer envelope.

3.1. Multi-Epoch Observations

For example, MERLIN observations of the 22 GHz masers of the Semi-Regular variable RT Vir were taken over six epochs over a ~ 3 month period by Richards et al. (1999). An unfilled ring structure indicates that the brightest maser emission is tangentially amplifying in this star (for stars of higher mass loss rate, radial amplification occurs). The average angular size of a maser component/feature is $2.3 \pm 1.0 \times 10^{13}$ cm. Richards et al. (1999) find that the components reside in a thick shell whose inner and outer radii and expansion velocities are given by: $r_i = 6.9 \times 10^{13}$ cm, $r_o = 28.8 \times 10^{13}$ cm; $v_i = 3.5 \text{ km s}^{-1}$, $v_o = 11.0 \text{ km s}^{-1}$. However, outflow deviates from spherical symmetry and it is possible that the star loses mass asymmetrically. They also conclude that H_2O masing clouds are about 50 times

denser than their surroundings, which is consistent with the data in Richards et al. (1996,1998).

3.2. H_2O Polarization

As for SiO, the Zeeman splitting of H_2O would be extremely small for the maximum field strengths likely in that region of the CSE (a few hundred mG), only $\approx 10^{-3}$ times the typical Gaussian linewidth of the H_2O maser line. However, it is possible to detect the splitting using high spectral resolution polarization observations and Vlemmings et al. (2001,2002) have made such measurements for several stars. The values they obtain are $\approx 150 \text{ mG} - 500 \text{ mG}$ for the 3 supergiants measured and for the Mira in their sample, U Her, $\approx 1.5 \text{ G}$. A non-Zeeman interpretation for H_2O circular polarization is given in Nedoluha & Watson (1990).

4. OH Masers

OH masers are located typically in the outer CSE, in the fully-developed stellar wind. In red giant winds, the OH maser mainlines at 1665 and 1667 MHz exist in the region $\sim 10^{15} - 10^{16}$ cm, whereas the 1612 MHz masers occur in larger shells at $\sim 10^{16}$ cm. OH 1612 MHz masers have double-peaked intensity profiles indicative of the radial ‘front-back’ amplification process, the velocity separation between the peaks centering on the stellar velocity (e.g., Booth et al. 1981). The incomplete and clumpy appearance of the OH maser shells indicates the deviations from pure spherical symmetry present also in this region of the CSE.

4.1. OH Polarization

Zeeman splitting of the OH lines shows the magnetic field strength in this relatively outer region of the CSE is $\approx 1 \text{ mG}$ for Miras (e.g. Szymczak & Cohen 1997). OH is paramagnetic and splitting is greater than the linewidth for conditions in the CSE. On the basis of the polarization measurements for all the three maser species, Vlemmings et al. (2002) favour a solar-type magnetic field structure for the CSEs of AGB stars.

5. Maser Simulations using dynamical stellar models

In order to investigate the effect of AGB stellar pulsation on stellar masers, Humphreys et al. (1996,2001,2002) couple SiO and H_2O maser models to a M-Mira hydrodynamic pulsation model Bowen (1998). In calculations performed around every two weeks during the cycle of the model star, VLBI and single-dish data can be well-reproduced qualitatively. SiO masers form in a tangentially amplifying ring within a few stellar radii. SiO single-dish lineshapes, of extent around 10 km s^{-1} , form a single dominant peak near the stellar velocity and maser emission from $v = 1 - v = 3$ up to $J = 10 - 9$ is found. Low-intensity linings, which exceed the outflow velocity, also occur as a phase-dependent phenomenon, from shocked gas in the extended atmosphere in a model which does not include rotation. Gray & Humphreys (2000) predict that the spatial separation

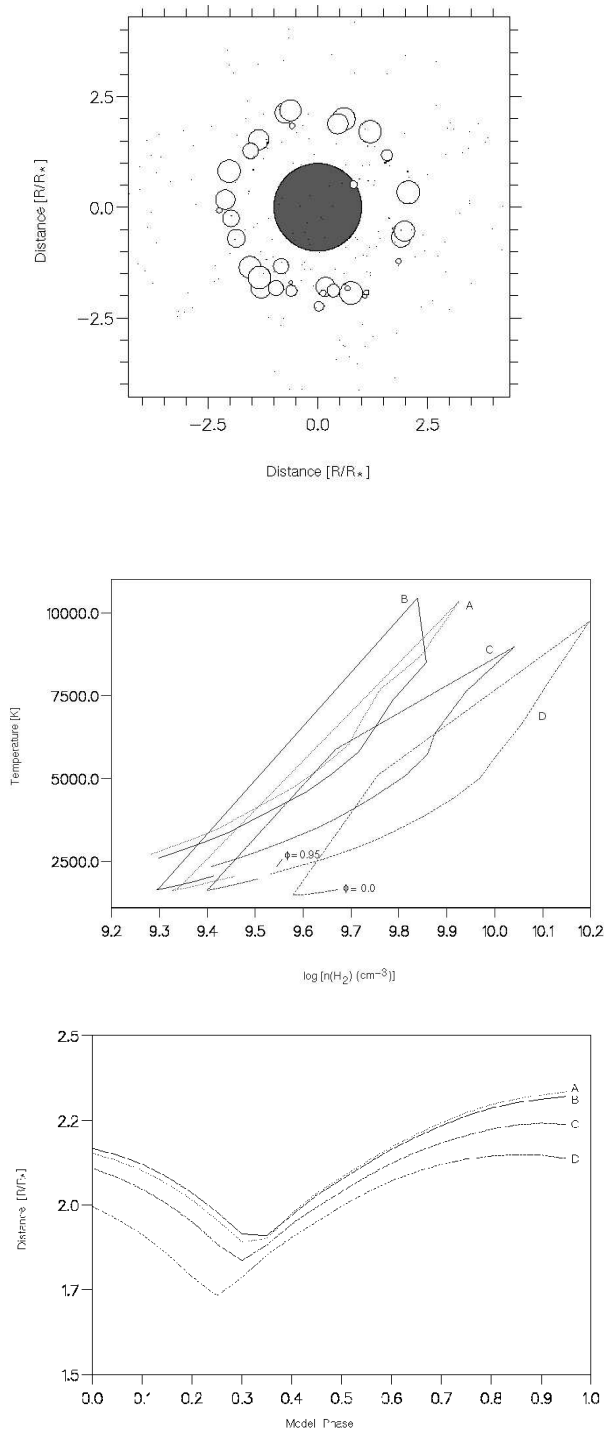


Fig. 3. a) (top) As for Fig. 1 except $\nu = 1 J = 1 - 0$ SiO masers (43 GHz); b) (middle) physical conditions encountered by four bright SiO components during the cycle; c) (bottom) accompanying motions within the CSE.

between the $\nu = 1$ & $2 J = 1 - 0$ maser rings is a stellar phase-dependent quantity, varying between 0.1 – 0.3 AU during the stellar cycle for a Mira-type star. Cotton et al. (2004) report that variations of ring diameter for most, but not all stars, had an rms amplitude in agreement with the simulations, but the expected relationship between the diameter and pulsation phase was not

seen. Many features of stellar H₂O masers are also reproduced, see Humphreys et al. (2001).

6. Outlook

Multi-epoch and polarization imaging of the masers in AGB stars provides invaluable data on the physical conditions in CSEs. We now have better prospects than ever for understanding the complex processes governing stellar winds and the mass-loss process of AGB stars.

The challenge is to interpret the observations in terms of the temperature, number density, dynamics and magnetic field structure of the stellar extended atmosphere and CSE. Maser observations may indicate the need to incorporate the effects of stellar magnetic fields, clump formation, non-spherical symmetry and perhaps rotation in AGB dynamical models. Further analyses are required in order to understand fully the cause of polarization for the SiO and H₂O maser emission, and the effect of potentially dynamically important magnetic fields in shaping the stars as they evolve along the AGB.

In connection to the status of circumstellar maser modeling and simulations, it is encouraging that existing simulations are now able to reproduce many observed characteristics of circumstellar maser emission. New generation maser codes, which calculate radiative transfer accurately (e.g. using Accelerated Lambda Iteration) for many level systems, are under development and hydrodynamical models which incorporate time-dependent dust formation and chemistry have been produced for O-rich stars. These developments will yield increasingly accurate model predictions for stellar masers.

References

- Alcolea, J., Pardo, J. R., Bujarrabal, V., Bachiller, R., Barcia, A., Colomer, F., Gallego, J. D., Gómez-González, J., del Pino Cisneros, A., Planesas, P., et al. 1999, A&AS, 139, 461
- Barvainis, R., McIntosh, G., Predmore, C. R. 1987, Nature, 329, 613
- Bieging, J.H., Shaked, S., Gensheimer, P. D. 2000, ApJ, 543, 897
- Blackman, E.G., Frank, A., Markiel, J.A., et al., 2001, Nature, 409, 585
- Boboltz, D., Diamond, P.J., Kemball, A.J. 1997, ApJ, 487, L147
- Boboltz, D.A., Diamond P.J. 2000, 197, 4507
- Boboltz, D.A., Marvel, K.B. 2000, ApJ, 545, L149
- Boboltz, D. A., Claussen, M. J., 2004, ApJ, 608, 480
- Booth, R., Norris, R.P., Porter, N.D., Kus, A.J. 1981, Nature, 290, 382
- Bowen, G. 1988, ApJ, 329, 299
- Bowers, P. F., Johnston, K. 1994, ApJS 92, 189
- Cernicharo, J., Bujarrabal, V., Santaren, J. L. 1993, ApJ, 407, L33
- Chapman, J.M., Cohen, R.J. 1986, MNRAS 220, 513
- Colomer, F., Graham, D. A., Krichbaum, T. P., et al. 1992, A&A, 254, L17
- Colomer, F., Reid, M.J., Menten, K.M., Bujarrabal, V. 2000, A&A 355, 979
- Cotton, W. D., Mennesson, B., Diamond, P. J., Perrin, G., Coudé du Foresto, V., Chagnon, G., van Langevelde, H. J., Ridgway, S., Waters, R., Vlemmings, W., et al. 2004, A&A, 414, 275
- Cuntz, M., Muchmore, D.O. 1994, ApJ, 433, 303
- Danchi, W. C., Bester, M., Degiacomi, C. G., Greenhill, L. J., Townes, C. H. 1994, AJ, 107, 1469
- Desmurs, J.F., Bujarrabal, V., Colomer, F., Alcolea, J. 2000, A&A, 360, 189

- Diamond, P.J., Kemball, A.J, Junor, W., et al. 1994, ApJ, 430, L61
Diamond, P. J. & Kemball, A. J. 1999, in IAU 191, 195
Diamond, P. J. & Kemball, A. J. 2001, in IAU 205, 252
Diamond, P. J. & Kemball, A. J. 2003, ApJ, 599, 1372
Doeleman, S.S., Lonsdale, C.J., Greenhill, L.J. 1998, ApJ, 494, 400
Dorch, S. B. F. 2004, A&A, 423, 1101
Elitzur, M. 1996, ApJ, 457, 415
González-Alfonso, E., Cernicharo, J., Alcolea, J., Orlandi, M.A. 1998, A&A 334, 1016
Gray, M.D. & Humphreys, E.M.L. 2000, New Ast., 5, 155
Gray, D. F. 2003, 'The Future of Cool Stars Workshop', p344
Gray, M.D. 2003, MNRAS, 343, L43
Greenhill, L.J., Colomer, F., Moran, J.M., et al. 1995, ApJ, 449, 365
Hartquist, T.W., Dyson, J.E. 1997, A&A, 319, 589
Herpin, F., Baudry, A., Thum, C., Morris, D., Wiesemeyer, H. 2003, Sf2A-2003,p523
Hollis, J. M., Boboltz, D. M., Pedelty, J. A., et al. 2001, ApJ, 559, L37
Humphreys, E.M.L., Gray, M.D., Yates, J.A., et al. 1996, MNRAS 282, 1359
Humphreys, E.M.L., Yates, J.A., Gray, M.D., Field, D., Bowen, G. 2001, A&A 379, 501
Humphreys, E.M.L., Gray, M.D., Yates, J.A., et al. 2002, A&A 286, 256
Kemball, A.J. & Diamond, P. J. 1997, ApJ, 481, L111
Menten, K.M., Melnick, G.J., Phillips, T.G., Neufeld, D.A. 1990, ApJ 363, L27
Menten, K.M., Melnick, G.J. 1991, ApJ 377, 647
Nedoluha, G.E., Watson, W.D. 1990, ApJ, 361, L53
Pardo, J. R., Cernicharo, J., González-Alfonso, E., Bujarrabal, V. 1998, A&A, 329, 219
Pardo, J. R., Alcolea, J., Cernicharo, J., Bujarrabal, V., Colomer, F., del Romero, A., de Vicente, P. 2004, A&A, 424, 145
Perrin, G., Ridgway, S. T., Coudé du Foresto, V., Mennesson, B., Traub, W. A., Lacasse, M. G. 2004, 418, 675
Phillips, R. B., Straughn, A. H., Doeleman, S. S., Lonsdale, C. J. 2003, ApJ, 588, L105
Reid, M.J., Menten, K.M. 1990, ApJ 360, L51
Reid, M.J. & Menten, K.M., 1997, ApJ, 476, 327
Richards, A.M.S., Yates, J.A., Cohen, R.J. 1996 MNRAS 282, 665
Richards, A.M.S., Yates, J.A., Cohen, R.J. 1998 MNRAS 299, 319
Richards, A. M. S., Cohen, R. J., Bains, I. 1999, in IAU 191, 315
Schwarzschild, M. 1975, ApJ 195, 137
Szymczak, M., Cohen, R.J. 1997, MNRAS, 288, 945
Tuthill, P. G., Haniff, C. A., Baldwin, J. E. 1997, MNRAS 285, 529
Tuthill, P.G., Monnier, J. D., Danchi, W. C. 1999, IAU 191, p.331
Vlemmings, W., Diamond, P. J., van Langevelde, H. J. 2001, A&A, 375, L1
Vlemmings, W., Diamond, P. J., van Langevelde, H. J. 2002, A&A, 394, 589
Western, L. R. & Watson, W. D. 1983, ApJ, 275, 195
Wiebe, D. S., Watson, W. D. 1998, ApJ, 503, L71
Woitke, P., Sedlmayr, E., Lopez, B. 2000, A&A, 358, 665
Yates, J.A., Cohen, R.J. 1994, MNRAS 270, 958
Yates, J.A., Cohen, R.J., Hills, R.E. 1995, MNRAS 273, 529
Yi, J., Booth, R.S., Conway, J.E., et al. 2002, in IAU 206, 274